Substructure Synthesis: A Controls Approach

Peiman G. Maghami * and Kyong B. Lim †
NASA Langley Research Center, Hampton, VA 23681

Substructure synthesis from a controls perspective is considered. An efficient and computationally robust method for synthesis of substructures is developed. The method considers the interface forces/moments as control inputs and redefines the synthesis problem in terms of obtaining a constant gain compensator which would ensure the connectivity requirements of the combined structure. Orthogonal similarity transformations are used to provide simplified synthesized dynamics of the combined system. The simplicity of form in transformed coordinates are exploited to effectively deal with modeling parametric and non-parametric uncertainties at substructure level. Uncertainty models of reasonable size and complexity are derived for the combined structure from those in the substructure models.

Introduction

Substructure synthesis is a well established area in the modeling of flexible structures as is evident in the voluminous literature of which a sample of tutorial papers are given in [1-6]. It is concerned with the modeling of the structural dynamics of substructures (or components) and then synthesizing them to predict the combined structural response. This synthesis is accomplished by enforcing deflection compatibility and force equilibrium at all substructure interfaces. There are several advantages of modeling via substructure synthesis, among these, (1) it allows much independence in the design and analysis of substructures, which is especially helpful if substructures are designed, fabricated, and even tested by different organizations. An example is the damping synthesis for the Space Shuttle[7] and more recently the component modules for the International Space Station which are built by different companies in several countries. (2) it increases the power of existing finite-element analysis and design programs by allowing analysis/design by components especially in problems where too many finite element degrees of freedom are required to perform a dynamic analysis/design of the complete system. (3) It allows a direct synthesis of substructure test data. This is particularly useful for very large structural systems (such as the International Space Station) that cannot be tested as a whole. This also means that it can be used as a part of an experimental verification tool for substructures before deployment as a connected structure.

Since its earliest work in,[1] the primary goal of substructure synthesis methods has not changed, i.e. to accurately predict the combined modal parameters: structural resonant frequencies and mode shapes. Consistent with the primary goal, most attention has been given to the issue of selecting a most effective subset of component (or assumed) modes and the related issue of modeling the substructure interfaces. Thus, relatively little attention has been given to issues germane to active control.

In this paper, we re-examine the substructure synthesis method from a controls perspective. In particular, our end goal is to develop a physically realistic and highly efficient way of modeling and controlling large flexible structures based on substructure (subsystems) models. As in any studies in multivariable control, we are concerned with the issues of closed loop stability and performance robustness due to inevitable modeling errors, configuration changes, or exogenous disturbances. Since the stability and robustness is strongly dependent on the degree of accuracy of the mathematical model to the physical structure, we also examine the issues of modeling uncertainties for the substructures and their influence on the output of the connected structure.

Substructure Synthesis

For simplicity of presentation, consider two components, shown in Fig. 1, that have to be synthesized. Consider the interface forces and moments (between the two components) as control input forces yet to be determined. Moreover, assume that collocated and compatible with the interface forces/moments are linear/angular velocity outputs from each component. With these considerations, the linear and time-invariant dynamics of the two components are represented as follows

component 1

*Senior Research Engineer, Guidance and Control Branch, Senior Member AIAA.

†Senior Research Engineer, Guidance and Control Branch.

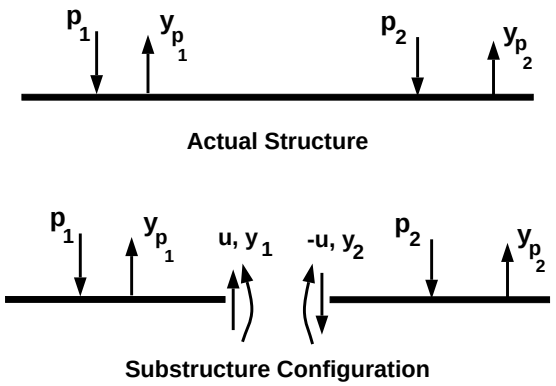

Fig. 1 Synthesized substructures

$$M_1\ddot{z}_1 + D_1\dot{z}_1 + K_1 z_1 = \tilde{B}_1 u + \tilde{H}_1 p_1 \tag{1}$$

$$y_1 = \tilde{C}_{r_1}\dot{z}_1 \tag{2}$$

$$y_{p_1} = \tilde{L}_{d_1} z_1 + \tilde{L}_{r_1}\dot{z}_1 + \tilde{L}_{a_1}\ddot{z}_1 \tag{3}$$

component 2

$$M_2\ddot{z}_2 + D_2\dot{z}_2 + K_2 z_2 = -\tilde{B}_2 u + \tilde{H}_2 p_2 \tag{4}$$

$$y_2 = \tilde{C_{r_2}}\dot{z}_2 \tag{5}$$

$$y_{p_2} = \tilde{L}_{d_2} z_2 + \tilde{L}_{r_2}\dot{z}_2 + \tilde{L}_{a_2}\ddot{z}_2 \tag{6}$$

where, for component i, z_i denotes the displacement vector; M_i is the positive definite inertia matrix; D_i is the damping matrix; K_i is the non-negative definite stiffness matrix; $\tilde{B}_i$ is the influence matrix for the interface forces/moments; u is the interface force/moment vector; y_i is the interface velocity vector; $\tilde{C}_{r_i}$ is the corresponding output influence matrix; y_{p_i} is the performance output vector; which could be a combination of displacement, velocity, and acceleration outputs; and $\tilde{L}_{d_i}$, $\tilde{L}_{r_i}$, and $\tilde{L}_{a_i}$ are the corresponding influence matrices. Since the order of a large flexible space structure (LFSS) can be quite large, for design and analysis purposes the order of the system is reduced to a design size using model reduction techniques such as modal truncation or modal cost analysis to obtain for component i, i=1,2

$$M_{r_i}\ddot{q}_{r_i} + D_{r_i}\dot{q}_{r_i} + K_{r_i} q_{r_i} = \pm {\Phi_i}^T \tilde{B}_i u + {\Phi_i}^T \tilde{H}_i p_i \tag{7}$$

$$y_i = \tilde{C}_{r_i}\Phi_i\dot{q}_{r_i} \tag{8}$$

$$y_{p_i} = \tilde{L}_{d_i}\Phi_i q_{r_i} + \tilde{L}_{r_i}\Phi_i\dot{q}_{r_i} + \tilde{L}_{a_i}\Phi_i\ddot{q}_{r_i} \tag{9}$$

where q_{r_i} is the vector of modal amplitudes obtained from transformation $z_i = \Phi_i q_{r_i}$; M_{r_i}, D_{r_i}, K_{r_i} are, respectively, the generalized inertia, damping and stiffness matrices; and Φ_i is a matrix whose columns are the r open-loop eigenvectors associated with the included modes. If the mode shapes are normalized with respect to the inertia matrix, and modal damping is assumed, then $M_{r_i} = I_{r\times r}$, $D_{r_i} = Diag\{2\zeta_{1_i}\omega_{1_i}, \ldots, 2\zeta_{r_i}\omega_{r_i}\}$, and $K_{r_i} = Diag\{\omega_{1_i}^2, \ldots, \omega_{r_i}^2\}$, where ω_{j_i} and ζ_{j_i}, $j = 1, \ldots, r$ are the open-loop frequencies and damping ratios for the ith component. Defining the state vector $x_i = \{\ q_{r_i} \quad \dot{q}_{r_i}\ \}^T; i = 1, 2$, the second-order dynamics of the components can be rewritten in first-order forms as follows

component 1

$$\dot{x}_1 = A_1 x_1 + B_1 u + H_1 p_1 \tag{10}$$

$$y_1 = C_1 x_1 \tag{11}$$

$$y_{p_1} = L_1 x_1 + D_{u_1} u + D_{p_1} p_1 \tag{12}$$

component 2

$$\dot{x}_2 = A_2 x_2 + B_2 u + H_2 p_2 \tag{13}$$

$$y_2 = C_2 x_2 \tag{14}$$

$$y_{p_2} = L_2 x_2 + D_{u_2} u + D_{p_2} p_2 \tag{15}$$

where A_i, B_i, H_i, C_i, and L_i, $i = 1, 2$, respectively denote the state matrix, input influence (interface forces or moments) matrix, exogenous disturbances influence matrix, velocity output influence matrix, and non-interface output influence matrix for each component. The matrices D_{u_1}, D_{p_1}, D_{u_2}, and D_{p_2}, represent feedthrough matrices associated with non-interface outputs of each component; x_1 and x_2 denote the state vectors of the components; y_1 and y_2 denote the interface velocity output vectors; y_{p_1} and y_{p_2} denote the non-interface output vectors components; and p_1 and p_2 represent the exogenous disturbances acting on the components. The system matrices in the first-order forms are related to those in second-order forms as follows:

$$A_i = \begin{bmatrix} 0 & I \\ -K_{r_i} & -D_{r_i} \end{bmatrix} \ ; \ B_i = \begin{bmatrix} 0 \\ \pm {\Phi_i}^T \tilde{B}_i \end{bmatrix} \tag{16}$$

$$H_i = \begin{bmatrix} 0 \\ {\Phi_i}^T \tilde{H}_i \end{bmatrix} \; ; \; C_{r_i} = \begin{bmatrix} 0 & \tilde{C}_{r_i}\Phi_i \end{bmatrix}; \qquad (17)$$

$$L_i = \begin{bmatrix} \tilde{L}_{d_i}\Phi_i - \tilde{L}_{a_i}\Phi_i K_{r_i} & \tilde{L}_{r_i}\Phi_i - \tilde{L}_{a_i}\Phi_i D_{r_i} \end{bmatrix} \qquad (18)$$

$$D_{u_i} = \pm\tilde{L}_{a_i}\Phi_i{\Phi_i}^T\tilde{B}_i \quad ; \quad D_{p_i} = \tilde{L}_{a_i}\Phi_i{\Phi_i}^T\tilde{H}_i \qquad (19)$$

Now, for the two components to be connected, in a dynamical sense, one has to find a control input vector u, representing the internal forces and moments at the interface, such that the displacements and rotations of the two components at the interface remain identically the same for all p_1 and p_2, and all compatible initial conditions. To achieve this, append the dynamics of the components, to obtain

$$\begin{Bmatrix} \dot{x}_1 \\ \dot{x}_2 \end{Bmatrix} = \begin{bmatrix} A_1 & 0 \\ 0 & A_2 \end{bmatrix} \begin{Bmatrix} x_1 \\ x_2 \end{Bmatrix} + \begin{bmatrix} B_1 \\ B_2 \end{bmatrix} u + \begin{bmatrix} H_1 & 0 \\ 0 & H_2 \end{bmatrix} \begin{Bmatrix} p_1 \\ p_2 \end{Bmatrix} \qquad (20)$$

$$y \equiv y_1 - y_2 = \begin{bmatrix} C_1 & -C_2 \end{bmatrix} \begin{Bmatrix} x_1 \\ x_2 \end{Bmatrix} \qquad (21)$$

$$y_p \equiv \begin{Bmatrix} y_{p_1} \\ y_{p_2} \end{Bmatrix} = \begin{bmatrix} L_1 & 0 \\ 0 & L_2 \end{bmatrix} \begin{Bmatrix} x_1 \\ x_2 \end{Bmatrix} + \begin{bmatrix} D_{u_1} \\ D_{u_2} \end{bmatrix} u + \begin{bmatrix} D_{p_1} & 0 \\ 0 & D_{p_2} \end{bmatrix} \begin{Bmatrix} p_1 \\ p_2 \end{Bmatrix} \qquad (22)$$

The new output vector y is the difference between the velocity of the two components at their interface. The problem is to find u such that y is identically zero for all p_1 and p_2, and compatible $x_1(0)$ and $x_2(0)$. From Eq. (21), for y to remain identically zero for all p_1 and p_2, $\begin{Bmatrix} x_1 \\ x_2 \end{Bmatrix}$ must remain identically in the right null space of the matrix $\begin{bmatrix} C_1 & -C_2 \end{bmatrix}$. This means that an appropriate control vector u must be found that would render the system identically unobservable, i.e., $\begin{Bmatrix} x_1 \\ x_2 \end{Bmatrix}$ identically remains in the undetectable subspace of the system given in Eqs. (20) and (21) for all p_1 and p_2. Let N_c denote an orthonormal basis for the right null space of $\begin{bmatrix} C_1 & -C_2 \end{bmatrix}$, i.e.,

$$\begin{bmatrix} C_1 & -C_2 \end{bmatrix} N_c = 0 \qquad (23)$$

and let R_c denote an orthonormal complement to N_c. Transform the system in Eq. (20) via an orthogonal similarity transformation, such that

$$\begin{Bmatrix} x_1 \\ x_2 \end{Bmatrix} = \begin{bmatrix} N_c & R_c \end{bmatrix} \begin{Bmatrix} \alpha \\ \beta \end{Bmatrix} \qquad (24)$$

The dynamics of the system in new coordinates becomes

$$\begin{Bmatrix} \dot{\alpha} \\ \dot{\beta} \end{Bmatrix} = \begin{bmatrix} \hat{A}_1 & \hat{A}_2 \\ \hat{A}_3 & \hat{A}_4 \end{bmatrix} \begin{Bmatrix} \alpha \\ \beta \end{Bmatrix} + \begin{bmatrix} \hat{B}_1 \\ \hat{B}_2 \end{bmatrix} u + \begin{bmatrix} \hat{H}_1 \\ \hat{H}_2 \end{bmatrix} p \qquad (25)$$

where $p = \begin{Bmatrix} p_1 \\ p_2 \end{Bmatrix}$ and

$$\begin{bmatrix} \hat{A}_1 & \hat{A}_2 \\ \hat{A}_3 & \hat{A}_4 \end{bmatrix} = \begin{bmatrix} N_c & R_c \end{bmatrix}^T \begin{bmatrix} A_1 & 0 \\ 0 & A_2 \end{bmatrix} \begin{bmatrix} N_c & R_c \end{bmatrix} \qquad (26)$$

$$\begin{bmatrix} \hat{B}_1 \\ \hat{B}_2 \end{bmatrix} = \begin{bmatrix} N_c & R_c \end{bmatrix}^T \begin{bmatrix} B_1 \\ B_2 \end{bmatrix} \qquad (27)$$

$$\begin{bmatrix} \hat{H}_1 \\ \hat{H}_2 \end{bmatrix} = \begin{bmatrix} N_c & R_c \end{bmatrix}^T \begin{bmatrix} H_1 & 0 \\ 0 & H_2 \end{bmatrix} \qquad (28)$$

Note that the linear and angular velocities at the interface are collocated and compatible with the forces and moments, i.e., $C_1 = B_1^T$ and $-C_2 = B_2^T$, such that along with Eq. (23), one has

$$N_c^T \begin{bmatrix} B_1 \\ B_2 \end{bmatrix} = N_c^T \begin{bmatrix} C_1 & -C_2 \end{bmatrix}^T = 0 \qquad (29)$$

resulting in

$$\hat{B}_1 = N_c^T \begin{bmatrix} B_1 \\ B_2 \end{bmatrix} = 0 \qquad (30)$$

Now, the control input vector u must be chosen such that $\beta(t)$, which represents the coordinates incompatible with the connectivity of the two components, remains identically zero for all t, p, and "compatible" initial conditions, i.e., $\beta(0) = 0$. To accomplish this, the input vector u must be chosen to render β unreachable from p, that is

$$u = -\hat{B}_2^{-1}[\hat{A}_3\alpha + \hat{H}_2 p] \qquad (31)$$

Note that the feedback gain associated with α and the feedthrough term associated with p must be in the form given in Eq. (31) to render β unreachable from p. Although, any u in the form of $u = -\hat{B}_2^{-1}[\hat{A}_3\alpha + \hat{H}_2 p] + R\beta$, with R as a non-destabilizing arbitrary matrix, would also be feasible, the condition for synthesizing the dynamics of the combined system necessitates that $\beta = 0$ for all t, thereby reducing the expression for u to that given in Eq. (31). The matrix inversion in Eq. (31) is guaranteed, as long as both input influence matrices B_1 and B_2 are full rank, which they are since

the interface forces are distinct. Therefore, since B_1 and B_2 are full rank, so is $\begin{bmatrix} B_1 \\ B_2 \end{bmatrix}$, and so is $\hat{B}_2$, since $\hat{B}_2 = R_C^T \begin{bmatrix} B_1 \\ B_2 \end{bmatrix}$, and R_c is an orthonormal basis for the column space of $\begin{bmatrix} B_1 \\ B_2 \end{bmatrix}$. Using the control input u of Eq. (31) in Eq. (25), with the aid of Eq. (30) simplifies to

$$\begin{Bmatrix} \dot{\alpha} \\ \dot{\beta} \end{Bmatrix} = \begin{bmatrix} \hat{A}_1 & \hat{A}_2 \\ 0 & \hat{A}_4 \end{bmatrix} \begin{Bmatrix} \alpha \\ \beta \end{Bmatrix} + \begin{bmatrix} \hat{H}_1 \\ 0 \end{bmatrix} p \qquad (32)$$

It is obvious from this equation that if the initial conditions are compatible, such that $\beta(0) = 0$, then β remains identically zero for all p and t, which means that, in the physical coordinates, $y_1 = y_2$ for all p and t. Therefore, compatibility conditions between the two components would be satisfied for all p and t. The synthesized dynamics of the combined system can be written in a reduced-order form in the transformed coordinates, or in the original component-based coordinates. In the transformed coordinates, these dynamics are given as follows

$$\dot{\alpha} = \hat{A}_1 \alpha + \hat{H}_1 p \qquad (33)$$

with the non-interface output defined from Eqs. (12), (15), (24), and (31)

$$y_p \equiv \begin{Bmatrix} y_{p_1} \\ y_{p_2} \end{Bmatrix} = \hat{N}_1 \alpha + \hat{D}_1 p \qquad (34)$$

where

$$\hat{N}_1 = \begin{bmatrix} L_1 & 0 \\ 0 & L_2 \end{bmatrix} N_c - \begin{bmatrix} D_{u_1} \\ D_{u_2} \end{bmatrix} \hat{B}_2^{-1} \hat{A}_3 \qquad (35)$$

$$\hat{D}_1 = \begin{bmatrix} D_{p_1} & 0 \\ 0 & D_{p_2} \end{bmatrix} - \begin{bmatrix} D_{u_1} \\ D_{u_2} \end{bmatrix} \hat{B}_2^{-1} \hat{H}_2 \qquad (36)$$

The dynamics of the combined system may also be presented in the original coordinates. Redefine the interface feedback law (Eq. (31)) in terms of the original coordinates, to obtain

$$\begin{aligned} u &= -\hat{B}_2^{-1} [\hat{A}_3 N_c^T \begin{Bmatrix} x_1 \\ x_2 \end{Bmatrix} + \hat{H}_2 p] \\ &\equiv - \begin{bmatrix} G_1 & G_2 \end{bmatrix} \begin{Bmatrix} x_1 \\ x_2 \end{Bmatrix} - \begin{bmatrix} D_1 & D_2 \end{bmatrix} \begin{Bmatrix} p_1 \\ p_2 \end{Bmatrix} \end{aligned} \qquad (37)$$

with the constant gain matrices G_1 and G_2, and the feedthrough terms D_1 and D_2 defined as

$$\begin{bmatrix} G_1 & G_2 \end{bmatrix} = \hat{B}_2^{-1} \hat{A}_3 N_c^T \;\; ; \;\; \begin{bmatrix} D_1 & D_2 \end{bmatrix} = \hat{B}_2^{-1} H_2$$

Using Eq. (37) in Eqs. (20) and (22), results in the combined dynamics of the two components in the original coordinates.

$$\begin{Bmatrix} \dot{x}_1 \\ \dot{x}_2 \end{Bmatrix} = \begin{bmatrix} A_1 - B_1 G_1 & -B_1 G_2 \\ -B_2 G_1 & A_2 - B_2 G_2 \end{bmatrix} \begin{Bmatrix} x_1 \\ x_2 \end{Bmatrix} + \begin{bmatrix} H_1 - B_1 D_1 & -B_1 D_2 \\ -B_2 D_1 & H_2 - B_2 D_2 \end{bmatrix} \begin{Bmatrix} p_1 \\ p_2 \end{Bmatrix} \qquad (38)$$

$$y_p = \begin{bmatrix} L_1 - D_{u_1} G_1 & -D_{u_1} G_2 \\ -D_{u_2} G_1 & L_2 - D_{u_2} G_2 \end{bmatrix} \begin{Bmatrix} x_1 \\ x_2 \end{Bmatrix} + \begin{bmatrix} D_{p_1} - D_{u_1} D_1 & -D_{u_1} D_2 \\ -D_{u_2} D_1 & D_{p_2} - D_{u_2} D_2 \end{bmatrix} \begin{Bmatrix} p_1 \\ p_2 \end{Bmatrix} \qquad (39)$$

Model Uncertainty

In this section, issues of parametric and nonparametric uncertainties in the component models and the way they effect the synthesized dynamics of the system will be considered. Parametric uncertainties include uncertainties in modal frequencies, damping ratios, and mode shapes of the components. The nonparametric uncertainties considered here are the unmodeled dynamics of the components. If modal models are used to represent the component dynamics, nonparametric uncertainties would be due to the truncated modes of the components. The development in this section uses the representation of the synthesized dynamics of the system in the transformed coordinates, as given in Eq. (33). This would make the treatment of parametric and nonparametric uncertainties easier. Here, only the case wherein there are no feedthrough terms (acceleration terms) associated with the non-interface outputs (see Eq. (34)), is considered. The treatment for the general case would be similar but more involved.

Uncertainty in Frequency and Damping

As mentioned earlier, the uncertainties in modal frequency and damping are embedded in the elements of the state matrices A_1 and A_2. One can represent these uncertainties via additive uncertainty blocks ΔA_1 and ΔA_2, such that the true state matrices are given by

$$A_1 \rightarrow A_1 + \Delta A_1 \qquad (40)$$

$$A_2 \rightarrow A_2 + \Delta A_2 \qquad (41)$$

Note that no assumption is made on the structure of the uncertainty blocks, ΔA_1 and ΔA_2, i.e., they can be structured or unstructured. Using Eqs. (40)-(41) in Eq. (33), and assuming that there are no uncertainties in the mode shape data and nonparametric

uncertainties present, one obtains the uncertainty representation in the transformed coordinates.

$$\dot{\alpha} = (\hat{A}_1 + \Delta\hat{A}_1)\alpha + \hat{H}_1 p \tag{42}$$

where

$$\Delta\hat{A}_1 = N_c^T \begin{bmatrix} \Delta A_1 & 0 \\ 0 & \Delta A_2 \end{bmatrix} N_c = N_{c_1}^T \Delta A_1 N_{c_1} + N_{c_2}^T \Delta A_2 N_{c_2} \tag{43}$$

N_{c_1} and N_{c_2} are column partition of N_c according to the components. This indicates that the additive parametric uncertainties in the component dynamics in the original coordinates carries through to the synthesized system in transformed coordinates, in the sense that it still remains in the form of an additive parametric uncertainty. However, it is observed from Eq. (43) that the structure of the uncertainty does not remain the same, its size decreases to match $\hat{A}_1$, but its bound remains invariant, since columns of N_c are orthonormal. In other words, $\Delta\hat{A}_1$ would have the same bounds as that of ΔA, i.e.,

$$|\Delta A| \leq \delta \quad \rightarrow \quad |\Delta\hat{A}_1| \leq \delta \tag{44}$$

The parametric uncertainty problem given in Eq. (43) may easily be put in a linear fractional representation (LFT) form for robust control design and/or analysis. Also, one could observe from Eq. (38) that, in this case, treating the uncertainty in the transformed coordinates would be cleaner and easier than treating it in the original coordinates.

Uncertainty in Mode Shapes

The parametric uncertainties in the mode shape data affect the elements of the input and output influence matrices, which include matrices C_1 and C_2. This means that there would be uncertainty associated with the elements of the basis vectors N_c, as seen form Eq. (23). Here we assume that the uncertainty in the mode shapes, whether structured or unstructured, can be translated into an uncertainty representation for N_c. With this assumption, the actual basis vectors N_c may be represented in various representations of uncertainty, such as additive, multiplicative, etc. Here, let N_c be represented as follows

$$N_c \rightarrow N_c + M_c\Delta \tag{45}$$

where M_c is a chosen basis for uncertainty influence, and Δ represent the uncertainty, which can be structured or unstructured. Using Eq. (45) in Eq. (33), and assuming that there are no uncertainties in the frequency and damping data or nonparametric uncertainties present, one obtains

$$\dot{\alpha} = (\hat{A}_1 + \Delta\hat{A}_1)\alpha + (\hat{H}_1 + \Delta^T M_c^T H)p \tag{46}$$

$$y_p = (\hat{N}_1 + LM_c\Delta)\alpha \tag{47}$$

where

$$\Delta\hat{A}_1 = \Delta^T M_c^T A M_c \Delta + \Delta^T M_c^T A N_c + N_c^T A M_c \Delta \tag{48}$$

$$A = \begin{bmatrix} A_1 & 0 \\ 0 & A_2 \end{bmatrix};\ H = \begin{bmatrix} H_1 & 0 \\ 0 & H_2 \end{bmatrix};\ L = \begin{bmatrix} L_1 & 0 \\ 0 & L_2 \end{bmatrix} \tag{49}$$

From these equations, it is observed that the input and output parametric uncertainties in the dynamics of the components, in the original coordinates, diffuse into input, output, and state parametric uncertainties in the transformed coordinates representation of the synthesized system dynamics. Moreover, the state parametric uncertainties involve a quadratic form of the uncertainty Δ. This form of uncertainty can be dealt with the technique presented in [8-9], wherein polynomial uncertainty representations are represented in optimal linear fractional representation (LFT) form approximations. The remaining uncertainties given in Eqs. (46) and (47) may easily be put in a linear fractional representation (LFT) form for robust control design and/or analysis.

Unmodeled Dynamics

The traditional approach in substructure synthesis has been to use higher bandwidth in the dynamics of the components to be synthesized, roughly twice the bandwidth of interest for the combined structure. This approach has worked successfully in many applications. However, it is somewhat ad hoc, with some potential shortcomings. First, it does not provide guaranteed levels of accuracy for the predicted system parameters, such as frequencies, damping ratios, etc. Second, it may suffer from finite element method's potential loss of numerical accuracy for higher frequency modes in addition to a loss of correlation with measured frequencies. As mentioned earlier, control design requires accurate assessment of model parameters or potential uncertainties. Traditionally, unmodeled dynamics, which typically include the higher frequency modes not included in the design model, have been treated via additive uncertainties in the plant model, which forces the control system to roll off to avoid potentially destabilizing spillover problems. Unfortunately, unmodeled (truncated) dynamics at the component level generally do not correspond to the same in the synthesized (combined) system. Consequently, it is imperative that the effects of unmodeled dynamics in the components be characterized at the system level for proper dynamics and controls design and analysis.

The approach taken here is similar to the treatment for parametric uncertainty, which essentially considered the effects of uncertainty in the transformed coordinates. Rewrite the dynamics of the components, including the unmodeled dynamics, in a first-order form.

component i= 1 or 2

$$\left\{ \begin{array}{c} \dot{x}_i \\ \dot{\overline{x}}_i \end{array} \right\} = \left[\begin{array}{cc} A_i & 0 \\ 0 & \overline{A}_i \end{array} \right] \left\{ \begin{array}{c} x_i \\ \overline{x}_i \end{array} \right\} + \left[\begin{array}{c} B_i \\ \overline{B}_i \end{array} \right] u + \left[\begin{array}{c} H_i \\ \overline{H}_i \end{array} \right] p_i \tag{50}$$

$$y_i = \left[\begin{array}{cc} C_i & \overline{C}_i \end{array} \right] \left\{ \begin{array}{c} x_i \\ \overline{x}_i \end{array} \right\} \tag{51}$$

$$y_{p_i} = \left[\begin{array}{cc} L_i & \overline{L}_i \end{array} \right] \left\{ \begin{array}{c} x_i \\ \overline{x}_i \end{array} \right\} \tag{52}$$

Here, the overbars indicate terms associated with the unmodeled dynamics. It should be noted that in most applications an accurate knowledge of the parameters associated with the unmodeled dynamics is not available, thus they are typically characterized in the form of uncertainty. Also, note that, similar to the previous treatments, the feedthrough terms in the non-interface outputs have been omitted. Following the synthesis procedure outlined previously, the component dynamics, as given in Eqs. (50)-(52), are appended to obtain a system similar to the one given by Eqs. (20)-(22), except that the order of the states are rearranged such that the modeled dynamics' states appear first, followed by the unmodeled dynamics' states, i.e., the state vector is given by $\left[\begin{array}{cccc} x_1^T & x_2^T & \overline{x}_1^T & \overline{x}_2^T \end{array} \right]^T$. Then, the space of feasible states (in the connectivity and compatibility sense) are characterized by an equation similar to Eq. (23), but for the expanded system, as follows

$$\left[\begin{array}{cccc} C_1 & -C_2 & \overline{C}_1 & -\overline{C}_2 \end{array} \right] N_c = 0 \tag{53}$$

Following the coordinate transformation (similar to Eq. (24)) and deriving the interface input vector u to guarantee the compatibility of the components' displacements and rotations at the interface, results in the synthesized dynamics of the combined system, which in transformed coordinates takes the form

$$\dot{\alpha} = \hat{A}_1 \alpha + \hat{H}_1 p \tag{54}$$

$$y_p = \hat{N}_1 \alpha \tag{55}$$

where

$$\hat{A}_1 = N_c^T \left[\begin{array}{cccc} A_1 & 0 & 0 & 0 \\ 0 & A_2 & 0 & 0 \\ 0 & 0 & \overline{A}_1 & 0 \\ 0 & 0 & 0 & \overline{A}_2 \end{array} \right] N_c \tag{56}$$

$$\hat{H}_1 = N_c^T \left[\begin{array}{cc} H_1 & 0 \\ 0 & H_2 \\ \overline{H}_1 & 0 \\ 0 & \overline{H}_2 \end{array} \right] \tag{57}$$

$$\hat{N}_1 = \left[\begin{array}{cccc} L_1 & 0 & \overline{L}_1 & 0 \\ 0 & L_2 & 0 & \overline{L}_2 \end{array} \right] N_c \tag{58}$$

It is reasonable to expect that both $\left[\begin{array}{cc} C_1 & -C_2 \end{array} \right]$ and $\left[\begin{array}{cccc} C_1 & -C_2 & \overline{C}_1 & -\overline{C}_2 \end{array} \right]$ are full rank. Define the null space of the matrix $\left[\begin{array}{cc} C_1 & -C_2 \end{array} \right]$ by the matrix N_{c_1}, whose columns are orthogonal. Then, it can easily be shown that the columns of matrix $\left[\begin{array}{c} N_{c_1} \\ 0 \end{array} \right]$ is included in the null space of $\left[\begin{array}{cccc} C_1 & -C_2 & \overline{C}_1 & -\overline{C}_2 \end{array} \right]$, represented by the matrix N_c, from Eq. (53). Now, choose and partition N_c, such that

$$N_c = \left[\begin{array}{cc} N_{c_1} & N_{\overline{c}_1} \\ 0 & N_{\overline{c}_2} \end{array} \right] \tag{59}$$

Here, the first column partition corresponds to the states of the modeled dynamics, and the second partition to the states of the unmodeled dynamics. Moreover, the first row partition corresponds to the null space of matrix $\left[\begin{array}{cc} C_1 & -C_2 \end{array} \right]$. Using Eq. (59) in Eqs. (54) and (55), and separating the states, gives

$$\dot{\alpha}_m = \tilde{A}_1 \alpha_m + \tilde{A}_2 \alpha_u + \tilde{H}_m p \tag{60}$$

$$\dot{\alpha}_u = \tilde{A}_3 \alpha_m + \tilde{A}_4 \alpha_u + \tilde{H}_u p \tag{61}$$

with

$$y_p = \tilde{N}_m \alpha_m + \tilde{N}_u \alpha_u \tag{62}$$

where

$$\left[\begin{array}{cc} \tilde{A}_1 & \tilde{A}_2 \\ \tilde{A}_3 & \tilde{A}_4 \end{array} \right] = \left[\begin{array}{cc} N_{c_1} & N_{\overline{c}_1} \\ 0 & N_{\overline{c}_2} \end{array} \right]^T \left[\begin{array}{cccc} A_1 & 0 & 0 & 0 \\ 0 & A_2 & 0 & 0 \\ 0 & 0 & \overline{A}_1 & 0 \\ 0 & 0 & 0 & \overline{A}_2 \end{array} \right] \left[\begin{array}{cc} N_{c_1} & N_{\overline{c}_1} \\ 0 & N_{\overline{c}_2} \end{array} \right] \tag{63}$$

$$\left[\begin{array}{c} \tilde{H}_m \\ \tilde{H}_u \end{array} \right] = \left[\begin{array}{cc} N_{c_1} & N_{\overline{c}_1} \\ 0 & N_{\overline{c}_2} \end{array} \right]^T \left[\begin{array}{cc} H_1 & 0 \\ 0 & H_2 \\ \overline{H}_1 & 0 \\ 0 & \overline{H}_2 \end{array} \right] \tag{64}$$

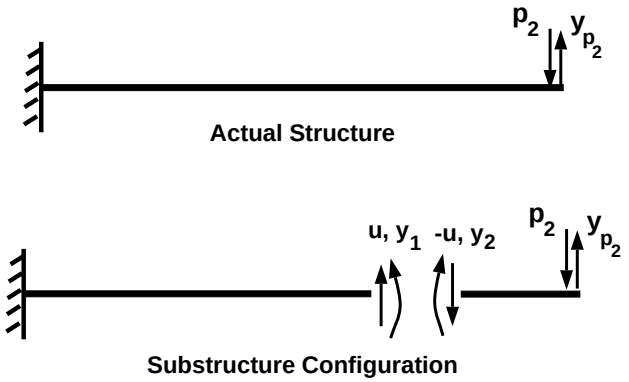

Fig. 2 Synthesized cantilevered beam problem

$$\begin{bmatrix} \tilde{N}_m & \tilde{N}_u \end{bmatrix} = \begin{bmatrix} L_1 & 0 & \overline{L}_1 & 0 \\ 0 & L_2 & 0 & \overline{L}_2 \end{bmatrix} \begin{bmatrix} N_{c_1} & N_{\overline{c}_1} \\ 0 & N_{\overline{c}_2} \end{bmatrix} \tag{65}$$

Note from Eq. (60) that $\tilde{A}_1$ is the same as $\hat{A}_1$ of the reduced dynamics for the baseline combined model (see Eq. (33)), so that if no unmodeled dynamics were present, Eq. (60) would represent the assembled structure. Furthermore, the state equations for α_m and α_u are coupled. One way of looking at this is to imagine that there are two systems, one attributed to the modeled dynamics (α_m states) and the other to the unmodeled dynamics (α_u states), which are in feedback connection. As mentioned earlier there are uncertainties associated with the unmodeled dynamics parameter, namely, $\tilde{A}_2$, $\tilde{A}_3$, $\tilde{A}_4$, $\tilde{H}_u$, and $\tilde{N}_u$, i.e., they are not known accurately. It can be said that the uncertainties, due to unmodeled dynamics, appear in feedback connection to the nominal plant. In other words, the uncertainties associated with unmodeled dynamics in the components, which are typically represented by additive uncertainty to the component models, takes the form of an uncertainty in a feedback loop with the nominal combined structure, when the synthesized dynamics are considered.

Numerical Results

The proposed methodology for substructure synthesis and controls is applied to a two-dimensional cantilevered beam problem to assess its effectiveness and feasibility. The current application involves substructure synthesis and does not include the substructure uncertainty treatment. The cantilevered beam is assumed to consist of two substructures, a cantilevered beam and a free-free beam, as indicated in Figure 2. The two interface forces/moments as well as the vertical displacement and slope are indicated, along with an exogenous disturbance at the tip of the second substructure. A performance output representing the tip deflection is also considered. The material and geometric properties of the system were chosen to provide considerable modal content in the low-mid frequency range to make the synthesis and control design task more challenging, and are provided in Table 1. The structure and its two substructures were modeled as Euler-Bernoulli beams. Each of the two substructures was modeled using the first 40 flexible modes, resulting in an 80th-order state space model for each of the substructures. The 40 modes used were deemed sufficient to provide a basis for describing the first 20 modes of the combined structure. The combined structure was also modeled using its first 20 modes, resulting in 40th-order state space model. This model was used for validation of the synthesis approach.

Table 1. Geometric and structural properties

Property	Substr. 1	Substr. 2	Whole
Length	150	50	200
Mass/Length	1000	1000	1000
Rigidity, EI	1.0e7	1.0e7	1.0e7
No. of modes	40	40	20

Using the procedure outlined in Eqs. (23)-(39), the dynamics of the two substructures were synthesized (combined), resulting in a 160th-order model in the original coordinates or a 158th-order model in transformed coordinates. Note that the synthesized model may be further reduced in order by using model reduction techniques, such as modal cost analysis or Hankel norm techniques. Table 2 compares the natural frequencies of the synthesized model vs. that of the validation (truth) model. Comparison of the frequencies indicate a good match between the two models, thus demonstrating the feasibility of the proposed synthesis technique. It should be pointed out that the degree of matching between any two frequencies in the table depends on whether the modal content used in the dynamics of each of the components provides a sufficient basis to express a mode at the system level.

Table 2. Natural frequencies

Mode No.	True	Synthesized
1	0.0088	0.0088
2	0.0551	0.0553
3	0.1542	0.1559
4	0.3022	0.3053
5	0.4996	0.5004
6	0.7464	0.7477
7	1.0425	1.0522
8	1.3879	1.4006
9	1.7827	1.7850
10	2.2268	2.2315
11	2.7203	2.7469
12	3.2631	3.2939
13	3.8553	3.8600
14	4.4968	4.5075
15	5.1877	5.2407
16	5.9279	5.9856
17	6.7175	6.7252
18	7.5564	7.5769
19	8.4447	8.5348
20	9.3823	9.4767

In order to obtain a better assessment of the appropriateness of the synthesized model, the Bode magnitude plots of the transfer function from the exogenous disturbance to the tip displacement were computed and are shown in Figure 3 for the synthesized and truth models. The two transfer functions agree very closely, as observed from Figure 3. Note that the peaks of the magnitude plots are finite although undamped models were used to compute the transfer function. The reason for the contradiction is the coarseness of the frequency points, i.e., no frequency point was chosen exactly at a resonance.

These results demonstrate the feasibility of the proposed synthesis approach.

Concluding Remarks

A novel and robust method for synthesizing the dynamics of substructures has been developed. The interface forces and moments were considered as control inputs, and used to design a constant gain compensator which synthesizes the combined dynamics of the substructures. The synthesized structure can be realized in original coordinates, or alternatively, in a transformed coordinates (obtained via orthogonal transformations). The realization of the system dynamics in transformed coordinates has the advantages

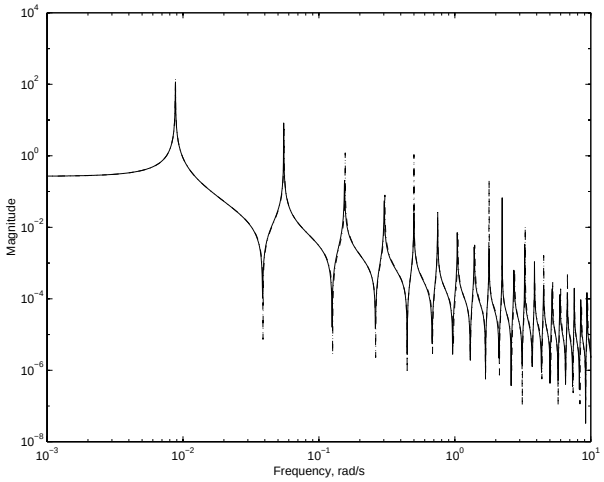

Fig. 3 Bode magnitude plot from exogenous disturbances to tip displacement; true(solid), synthesized(dashed)

of being more amenable to uncertainty and robustness analysis and design as well as being smaller in order. Using this realization, uncertainty models of reasonable size and complexity have been derived for the combined structure from parametric and nonparametric uncertainties in the substructure models. These models can and will be used for robust control design. An application of the proposed synthesis technique to a cantilevered beam problem demonstrated its feasibility.

References

[1]Hurty, W., "Vibrations of Structural systems by Component Mode Synthesis," *Journal of Engineering Mechanics Division, Proc. of ASCE*, 1960, pp. 51–69.

[2]Craig, R.R., J. and Bampton, M., "Coupling of Substructures for Dynamic Analysis," *AIAA Journal*, Vol. 6, No. 7, 1968, pp. 1313–9.

[3]Hintz, R., "Analytical Methods in Component Mode Synthesis," *AIAA Journal*, Vol. 13, No. 8, 1975, pp. 1007–16.

[4]Craig, R.R., J., "Methods of Component Mode Synthesis," *Shock and Vibration Digest*, Vol. 9, No. 11, 1977, pp. 3–10.

[5]Craig, R.R., J., *Structural Dynamics: Introduction to Computer Methods*, Wiley, 1981.

[6]Meirovitch, L. and Hale, A., "On the Substructure Synthesis Method," *AIAA Journal*, Vol. 19, No. 7, 1981, pp. 940–47.

[7]Kana, D. and Huzar, S., "Synthesis of Shuttle Vehicle Damping using Substructure Test Results," *AIAA Journal of Spacecraft and Rocket*, Vol. 10, Dec. 1973, pp. 790–7.

[8]Belcastro, C., "Parametric Uncertainty Modeling: An Overview," *Proc. of American Control Conference*, Philadelphia, PA, 1998, pp. 992–6.

[9]Belcastro, C., "On the Numerical Formulation of Parametric Linear Fractional Transformation (LFT) Uncertainty Models for Multivariate Matrix Polynomial Problems," Tm-1998-206939, NASA, Nov. 1998.